Case Study

Combined Impacts of Land Use and Climate Change in the Modeling of Future Groundwater Vulnerability

Lu Huang[1]; Guangming Zeng[2]; Jie Liang[3]; Shanshan Hua[4]; Yujie Yuan[5]; Xiaodong Li[6]; Haoran Dong[7]; Jiayu Liu[8]; Shuang Nie[9]; and Junfeng Liu[10]

Abstract: Groundwater vulnerability assessment delineating areas that are susceptible to contamination from future scenarios has aroused worldwide attention. In this study, the authors (1) estimate future groundwater vulnerability in Hunan province, China, under urban-related land-use change and climate change scenarios; and (2) analyze the importance of related parameters to future groundwater vulnerability. The DRASTIC model [including seven parameters: depth to water table (D), net recharge (R), aquifer type (A), soil type (S), topography (T), impact of vadose zone (I) and conductivity (C)] together with an extra parameter, land-use patterns, was used to generate the map of groundwater vulnerability in future scenarios. The results indicated that vulnerability classes had an increasing trend from low to high vulnerability in the future scenarios. Hunan province may face high groundwater pollution risk in the future. The sensitivity analysis indicated that the depth-to-water table may be the dominant factor, and the land-use pattern was the most sensitive parameter on the predicted future groundwater vulnerability in Hunan province. Decision makers should identify the potential future groundwater vulnerability and take early steps to protect groundwater resources. **DOI: 10.1061/(ASCE)HE.1943-5584.0001493.**

Author keywords: Groundwater vulnerability; Climate change; Land-use change; Urban; Intergovernmental Panel on Climate Change (IPCC); Hunan province.

Introduction

As an important supplement of drinking water, groundwater has become increasing prominent, especially in arid and semiarid regions where surface water is scarce (Kumar et al. 2014; Boy-Roura et al. 2013). However, groundwater quantity and quality are deteriorating in these regions due to the increase in urbanization and environmental change (Chen et al. 2010; Liang et al. 2010). Groundwater pollution prevention and control are of great importance. Groundwater vulnerability assessment is a useful tool in groundwater pollution prevention and control (Yuan et al. 2010; Huan et al. 2012). It provides a method for evaluating sensitivity of groundwater to contamination and scientifically defensible information for decision makers. Thus, it is essential in effectively preventing or reducing groundwater contamination.

Climate variables and land-use change factors are key factors in environmental change, which have been studied widely (Li et al. 2015; Liu et al. 2015). Therefore, the response of groundwater vulnerability to climate variables and land-use change factors cannot afford to be neglected (Kura et al. 2015; Zeng et al. 2013a). Climate change and urban-related land-use change are widespread problems in the process of groundwater vulnerability assessment (Lapworth et al. 2013; Stigter et al. 2014; Şen et al. 2013). Previous studies have recognized that scientifically, groundwater resource management should be based on reliable groundwater vulnerability assessment under a variety of possible future climate and urban-related land-use change scenarios. Changes in climate variables such as temperature, evaporation, and precipitation may lead to groundwater alterations. Anthropogenic activities, such as unsustainable water extraction for drinking and irrigation, emission of pollutants, and urbanization, would further exacerbate groundwater alterations (Pasini et al. 2012; Neukum and Azzam 2012; Xu et al. 2012; Gong et al. 2009). Many efforts have been devoted to analyze the effects of such processes and three significant points have been provided (Chae et al. 2004, 2002; Dimitriou and Moussoulis 2009; Zeng et al. 2009). First, climate change would directly affect groundwater vulnerability through interaction with surface-water resources, and net recharge and groundwater levels. Second, the potential pollution intensity varies since its assessment parameters can be greatly hampered by land-use patterns that involves agriculture, industry, commerce, and urban areas. Finally, urbanization often modifies the groundwater cycle and the induced changes may lead to a sharp decline or rise in groundwater level and deterioration in groundwater quality, thus enhancing the risk of pollution (Zeng et al. 2013b). Therefore, it is of great significance to focus on groundwater vulnerability that may be affected by both climate and

[1]Ph.D. Student, College of Environmental Science and Engineering, Hunan Univ., Changsha 410082, China. E-mail: hlu527@163.com

[2]Professor, College of Environmental Science and Engineering, Hunan Univ., Changsha 410082, China (corresponding author). E-mail: zgming@hnu.edu.cn

[3]Associate Professor, College of Environmental Science and Engineering, Hunan Univ., Changsha 410082, China. E-mail: liangjie@hnu.edu.cn

[4]Graduate Student, College of Environmental Science and Engineering, Hunan Univ., Changsha 410082, China. E-mail: hss20090310210@163.com

[5]Ph.D. Student, College of Environmental Science and Engineering, Hunan Univ., Changsha 410082, China. E-mail: yuanyujiehn@163.com

[6]Associate Professor, College of Environmental Science and Engineering, Hunan Univ., Changsha 410082, China. E-mail: lxdfox@163.com

[7]Associate Professor, College of Environmental Science and Engineering, Hunan Univ., Changsha 410082, China. E-mail: dongh@hnu.edu.cn

[8]Master, College of Environmental Science and Engineering, Hunan Univ., Changsha 410082, China. E-mail: liujiayu87@163.com

[9]Master, College of Environmental Science and Engineering, Hunan Univ., Changsha 410082, China. E-mail: 1095983288@qq.com

[10]Master, College of Environmental Science and Engineering, Hunan Univ., Changsha 410082, China. E-mail: 1501260160@qq.com

Note. This manuscript was submitted on February 21, 2016; approved on October 17, 2016; published online on March 10, 2017. Discussion period open until August 10, 2017; separate discussions must be submitted for individual papers. This paper is part of the ***Journal of Hydrologic Engineering***, © ASCE, ISSN 1084-0699.

land-use changes, especially in the region of a developing country. It provides important information of groundwater resource management to the government and facilities.

Existing methods used to assess groundwater vulnerability include the overlay index method, process simulation method, and statistical models (Babiker et al. 2005; Fan et al. 2008). Common overlay index methods include DRASTIC, SINTACS [including seven environmental variables: soil type (S), infiltration capacity (I), depth to water level (N), unsaturated zone (T), aquifer media (A), hydraulic conductivity (C) and slope (S)], aquifer vulnerability index (AVI), PI [protective cover (P), infiltration conditions (I)], and German state geological surveys (GLA) (Hernandez-Espriu et al. 2014). They superimpose the selected subindexes to calculate a composite index reflecting vulnerability extent (De Paz and Ramos 2002; Holman et al. 2004). Among them, the most widely used method is DRASTIC model for its distinct explanation, minimal data requirements, and easy-to-use flexibility (Masetti et al. 2009). This model was developed originally by the U.S. Environmental Protection Agency (1985) and has been applied extensively for vulnerability analyses across the globe, such as in India and China. Furthermore, the DRASTIC model has a low cost of application and can be applied across extensive regions. It has seven parameters, including depth to water table (D), net recharge (R), aquifer type (A), soil type (S), topography (T), impact of vadose zone (I), and conductivity (C). In addition, the obvious advantage of DRASTIC is that it can be adapted to other factors. For example, Li and Merchant (2013) used land use and land cover to represent a source of farm chemicals in groundwater. Shirazi et al. (2013) used land-use classification to represent the nitrate concentration in groundwater vulnerability.

As mentioned earlier, although many studies have assessed groundwater vulnerability, those studies were mainly focused on present scenarios or only climate change scenarios without consideration of urbanization. Little is known, however, about future groundwater vulnerability combining the effects of climate change and land-use change under an ensemble of climate change scenarios. The response of groundwater vulnerability to projected changes in climate change and urbanization is expected to be profound. Climate change and urbanization cannot be neglected during the process of groundwater vulnerability assessment. How to account for their effect and which one is the primary factor to affect groundwater vulnerability has long been under debate. This study predicts the future groundwater vulnerability under an ensemble of climate change scenarios and urbanization. Hunan province, in middle China, suffers from rapid urbanization and was used for the case study. The DRASTIC model was used to generate the map of groundwater vulnerability. An urban-related land-use pattern (L) that represents contamination impacts was considered as an additional DRASTIC parameter. The objectives of this study were (1) to estimate future groundwater vulnerability in the

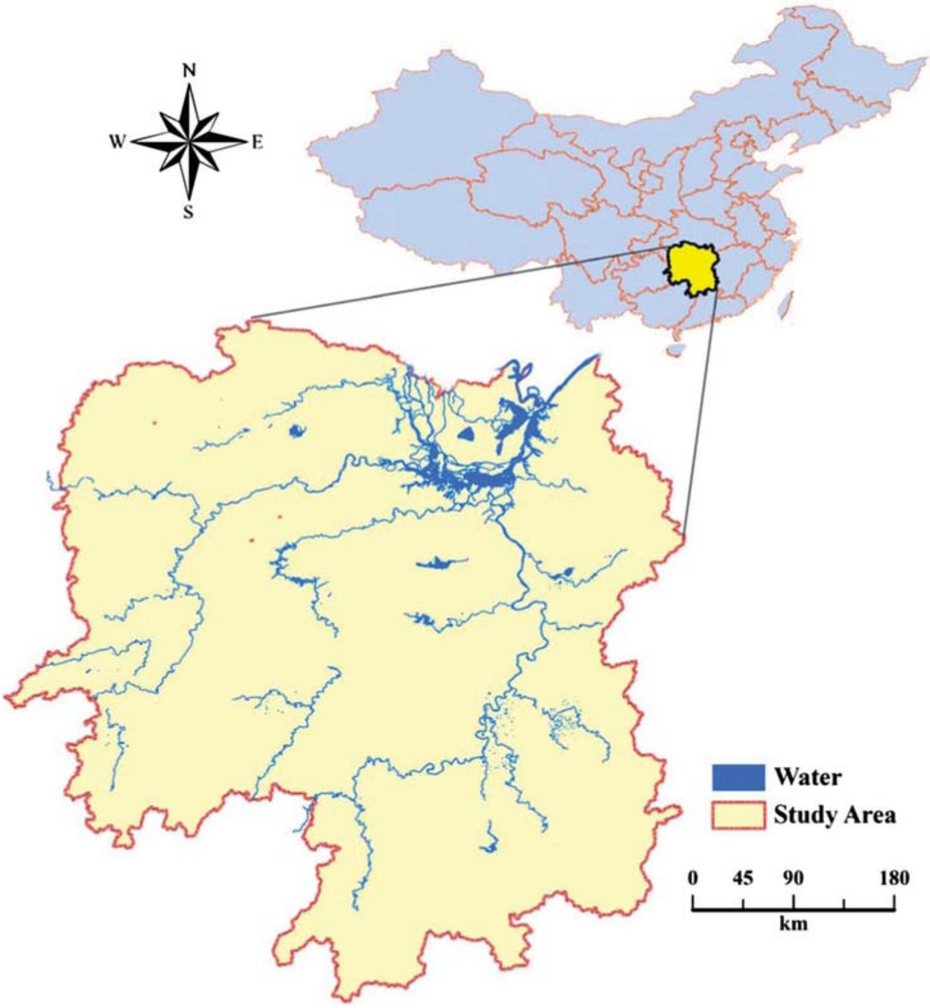

Fig. 1. Study area location in China and distribution of the major surface water within

study area under the ensemble of climate change scenarios and urbanization; and (2) to analyze the primary factor to affect future groundwater vulnerability.

Study Area

Hunan province is located in the middle of China. Covering an area of approximately 211,800 km^2, Hunan Province lies between 24°39′–30°28′ N and 108°47′–114°45′ E (Fig. 1). The region has a subtropical monsoon climate with an average annual sunshine of 1,300–1,800 h, an annual average temperature of 16–18°C, and mean annual precipitation of 1,200–1,700 mm. It has a continental climate typically with cold winters and hot summers. The mean altitude of Hunan province is 354 m above sea level. The rock formations consist mainly of limestone, sandstone, and gravel. The major section of the study area is formed by Eocene remains and consists mostly of alluvium and conglomerate. Hunan province has well-developed river system. China's second largest freshwater lake, Dongting Lake, is located in northern Hunan province. Dongting Lake is directly connected with the Yangtze River. The water from the Yangtze River flows into the lake via the Three Outfalls (Songzi River, Hudu River, and Ouchi River). The Xiangjiang, Zijiang, Yuanjiang, and Lishui Rivers converge on the Yangtze River (Changjiang River) at Lake Dongting in the north of Hunan.

In the study area, the unconfined aquifer was selected as the target for assessing vulnerability. In recent years, the unconfined aquifer has deteriorated gradually due to domestic, industrial, and agricultural pollution. Furthermore, increases in temperature, evaporation, and precipitation variations linked with global warming also changed the unconfined aquifer's vulnerability. With the double influence of human activities and global warming, climate variables and land-use change factors have become gradually the main factors responsible for groundwater vulnerability.

Material and Methods

In this study, the DRASTIC model was employed to estimate groundwater vulnerability in Hunan Province. An urban-related land-use pattern (L) was considered as an additional DRASTIC parameter to represent the potential of anthropogenic emissions of pollutants to groundwater due to rapid urbanization. Table 1 shows the assigned weights, ranges, and ratings of parameters D, R, A, S, T, I, C, and L. Weights were used to reflect the relative importance of the parameter in estimating groundwater vulnerability. Ratings are intended to reflect the relative significance of data values within each factor (Rahman 2008). The estimated groundwater vulnerability was calculated by weighted sum of the eight parameters using Eq. (1)

$$VI = D_w D_r + R_w R_r + A_w A_r + S_w S_r + T_w T_r + I_w I_r + C_w C_r + L_w L_r \quad (1)$$

where D, R, A, S, T, I, C, and L = eight parameters contributing to groundwater vulnerability; and subscripts w and r = corresponding weights and ratings.

Climate change would directly affect R and D. In addition, L would enhance the potential pollution risk of groundwater. The combined interactions of climate change and urban-related land-use patterns on groundwater vulnerability represent the main relationships between the primary natural and anthropogenic drivers (Fig. 2). Climate change and land-use pattern are simulated in the three future periods (years 2020, 2050, and 2080) under representative concentration pathways (RCP) scenarios proposed by the Intergovernmental Panel on Climate Change (IPCC) and a

Table 1. Weight, Range, and Rating of the DRASTIC Parameters and Land-Use Parameter

Rating	Depth to water table (D) (m)	Net recharge (R) (mm)	Aquifer media (A) (type)	Soil media (S) (type)	Topography (T) (%)	Impact of vadose zone (I) (type)	Hydraulic conductivity (C)	Land use (L)
	Weight: 5	Weight: 4	Weight: 3	Weight: 2	Weight: 1	Weight: 5	Weight: 3	Weight: 5
1	>30.5	0–51	—	Non-shrinking or non-aggregated clay	>18	Confined water	0.05–4.89	—
2	22.9–30.5	—	Shale	Backfill	—	—	4.89–14.67	Grass or forestry
3	15.2–22.9	51–102	Metamorphic rocks	Clay loam	12–18	Clay or mudstone	—	—
4	—	—	Igneous rocks	Silty loam	—	Metamorphic rocks	14.67–34.23	—
5	9.1–15.2	—	Till sheet	Loam	6–12	—	—	Water
6	—	102–178	Limestone, sandstone or gravel	Sandy loam	—	Limestone, sandstone or gravel	34.23–48.93	Plough land
7	4.6–9.1	—	—	Shrinking or aggregated clay	—	—	—	—
8	—	178–254	Conglomerate	Peat	—	Conglomerate	48.93–97.86	—
9	1.5–4.6	>254	Basalt	Sand	2–6	Basalt	—	Urban or other
10	0–1.5	—	Karst limestone	Gravel, thin or absent	0–2	Karst limestone	>97.86	—

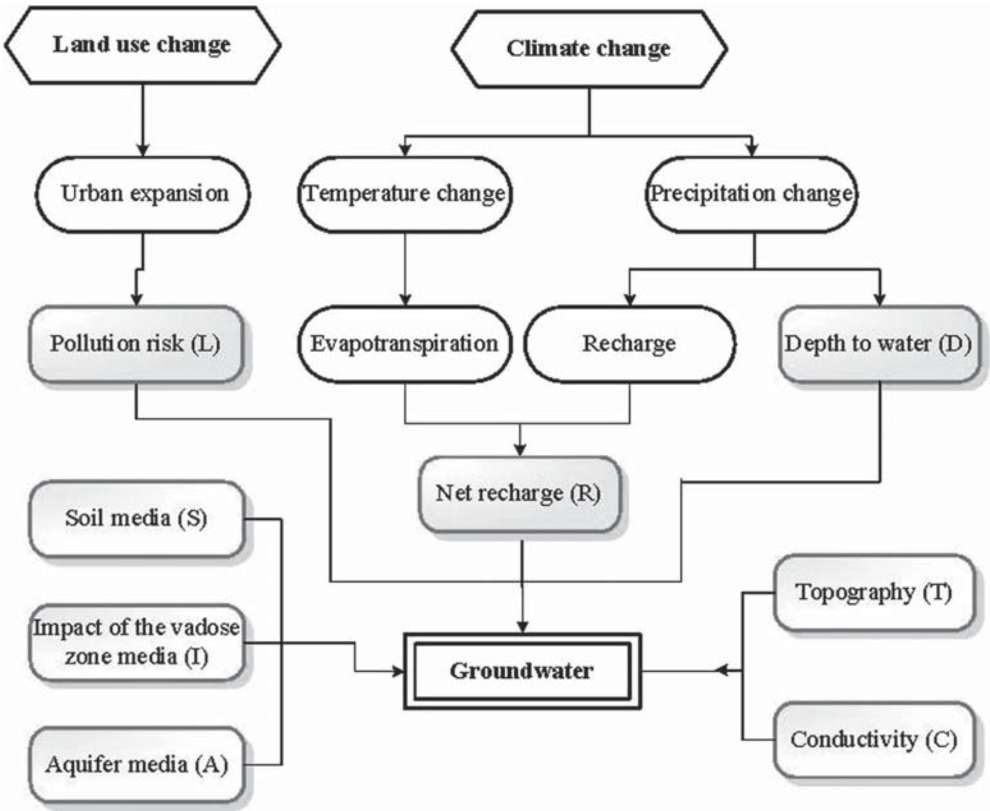

Fig. 2. Impact of climate change, land-use change, and environmental factors on groundwater

land transformation model (LTM). This paper will summarize the changing trends of future climate change scenarios, future groundwater net recharge, depth-to-water table change, and future urban-related land-use patterns.

The previous scenarios proposed by the IPCC Special Report (2013) *Special report on emission cenarios* (SRES) are based on four primary socioeconomic storylines, each having a different emphasis on economic growth, environmental management, and globalization. An RCP is assigned for each new scenario. The new RCP scenarios target fixed levels of radiative forcing by the year 2100 and are not based on any social or economic assumptions (Huang et al. 2008; Liang et al. 2015). The RCP scenario is divided into four types (RCP 2.6, 4.5, 6.0, and 8.5) depending on radiative forcing due to greenhouse gases. It is difficult to tell how likely each of the four climate scenarios is. Such probabilities depend on the implementation of a climate change mitigation policy, which is uncertain in nature (Ando and Mallory 2012). In this study, an ensemble climate change scenario, assuming each climate scenario is equally likely to occur, was adopted. Ensembles have been used to handle climate change scenario uncertainty in previous studies (Snover et al. 2013). Then the groundwater vulnerability parameters R and D for a baseline year 2000 and future years 2020, 2050, and 2080 under PCR were simulated.

Groundwater net recharge is the amount of water available to migrate down to the groundwater from precipitation and artificial sources (Boy-Roura et al. 2013). It is a significant means for percolating and transporting contaminants within the vadose zone to the saturated zone. Climate change will alter the hydrological cycle, inducing spatial and temporal changes in precipitation and evaporation. A number of studies have indicated that climate change can affect groundwater recharge (Gogu and Dassargues 2000; Raupach et al. 2013). The recharge map was constructed according to the following Eq. (2) (Kraller et al. 2012):

$$\Delta R = (C_{pre} - C_{eva} - C_{pum} - C_{irr}) \times R \qquad (2)$$

where ΔR = net recharge; C_{pre} = storage change in an aquifer by precipitation; C_{eva} = amount of water that is added to the aquifer less losses through evapotranspiration; C_{pum} = total groundwater abstraction by pumping; C_{irr} = total groundwater abstraction by irrigation, where all terms are in millimeters per unit time, or volume per unit aquifer area; and R = recharge rate representing groundwater drainage.

The precipitation and evaporation data were obtained by interpolating the year 2000 mean of annual precipitation (mm/year) from 24 representative rainfall stations. The recharge rate was assumed to be 85% for all the studied areas (Wu et al. 2014). The groundwater pumping and irrigation in Hunan were represented by zero providing recharge here, because pumping and irrigation are from surface-water resources (Fu et al. 2013). In this study, the projection data set was derived from the future precipitation and evaporation map in The IPCC's AR5 (fifth assessment report) assessment report. Currently, the National Climate Center provides regional climate data under the RCP scenarios (2011–2100) with 12.5-km grid spacing. (National Climate Center of China).

The depth-to-water table (DTW) is the distance between ground and groundwater table (Wang et al. 2012). It is one of the most important factors because it determines the thickness of material through which infiltrating water must travel before reaching the aquifer-saturated zone. The baseline data of depth-to-water table (DTW) were collected from the (China Statistical Yearbook 2013) *China groundwater level yearbook for geo-environmental monitoring*. Kriging interpolation was performed to generate the DTW map of Hunan Province.

DTW varies with many other parameters, such as net recharge. Forecasting the DTW in response to a change in climatic variables usually requires complex numerical modeling. (Ali et al. 2012). To simulate the future net recharge at a large scale, some assumptions must be proposed. In this study, two assumptions were provided in the modeling. That is, first, at any location, there was only one water table (neglecting local perched aquifers) (Tang et al. 2008; Fan et al. 2013). Second, at any location, the groundwater aquifer in Hunan was recharged mainly by direct infiltration from precipitation. The equation used to calculate DTW was as follows:

$$D = \Delta R(t_i) + H(t_i) \quad (3)$$

where $\Delta R(t_i)$ = net recharge occurring between initial time t_0 and ending time t_i; and $H(t_i)$ = baseline DTW attributed to the recharge period.

Future Urban-Related Land-Use Simulation

In this study, land-use pattern (L) was considered as an additional DRASTIC parameter to represent the potential of anthropogenic pollutant emissions to groundwater due to rapid urbanization. It was assumed that urbanization would first occur in a region suitable for construction and then occur in less-suitable regions (Hua et al. 2015). To estimate the future urban-related land-use patterns, a geographic information system (GIS)-based land transformation model (LTM) was employed (Pijanowski et al. 2002). This model can handle a variety of socioeconomic, political, and environmental inputs. The model essentially generates a suitability map for an urban area, and then selected the cells exhibiting the highest suitability to convert. The simulation focused only on urbanized areas.

In the study areas, five environmental variables were chosen as the driving factors for urban modeling in Hunan: distance to county roads, distance to a highway, distance to a lake, the distance to a river, and distance to the urban region in 1984. The authors chose these in consideration of the idea that the region being transformed to urban land should be close to an urban area and available infrastructure. For the purpose of ecological protection, the water area will remain the same during the modeling period. (Huang et al. 2013a). The model was calibrated and validated using 30 m-resolution land-use data obtained from the thematic mapper (TM) images for 1984 and 2000. The data from 1984 and 2000 in Hunan were used to project the

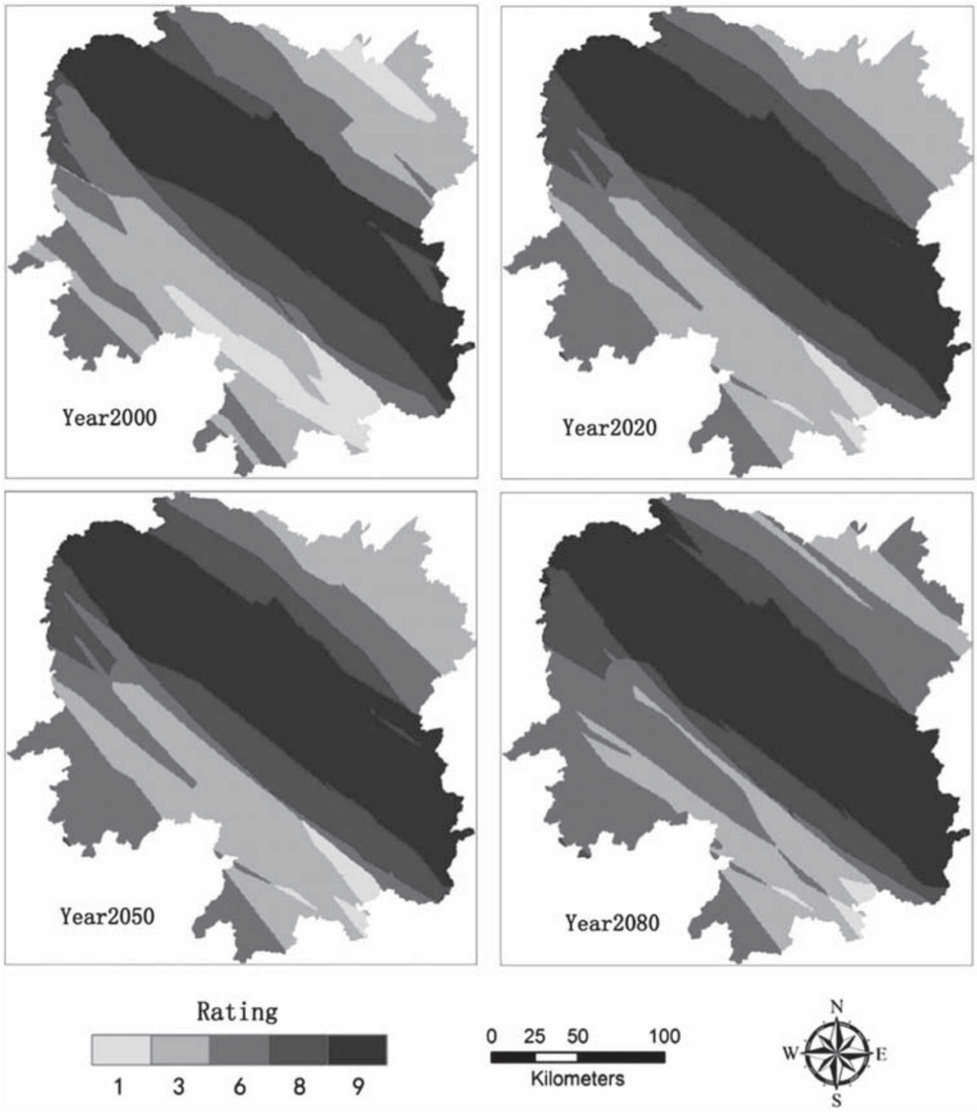

Fig. 3. Distribution of baseline (2000) and projected (2020, 2050, and 2080) groundwater net recharge under the climatic change scenarios in Hunan province

pattern of urban land in 2020, 2050, and 2080. The ratings and weights of the land use are given in Table 1.

Data Sources

An aquifer media is geological formation that contains sufficient saturated permeable material to yield significant quantities of water to wells or springs (Huang et al. 2013b; Neukum and Azzam 2012). The aquifer media parameter was prepared to use a subsurface geology map from National Geological Data Center of China (National Climate Center of China). The soil media parameter was prepared using a geological map from the Soil Survey and land-use Organization, Department of Agriculture, Hunan province. Topography of the study area was obtained from the digital elevation model (DEM) covering the study area (http://srtm.csi.cgiar.org/SELECTION/inputCoord.asp). Impact of the vadose zone was prepared from the lithological cross sections obtained from geophysical data from the National Geological Data Center of China (http://geodata.ngac.cn/). Hydraulic conductivity was calculated from the pumping test data of the boreholes and improved after calibration of the mathematical model in a steady state.

Results and Discussion

Fig. 3 shows the results of future scenarios of mean annual net recharge in the study area. The results indicate that climate change could affect groundwater net recharge greatly in most parts of Hunan province with increases ranging from 1 to 12 cm. Groundwater net recharge would increase moderately during 2020–2050 and dramatically during 2050–2080. The average net recharge in 2020, 2050, and 2080 were 17.1, 18.2, and 21.8 cm, respectively. The simulated results are consistent with the IPCC's climate change scenario. In the IPCC Special Report (2013), precipitation would have the highest increasing trend during the later period of the 21st century and evaporation would have a moderate trend during the whole 21st century. According to Eq. (2), projected future precipitation patterns are critical to the differences in net recharge between 2020–2050 and 2050–2080.

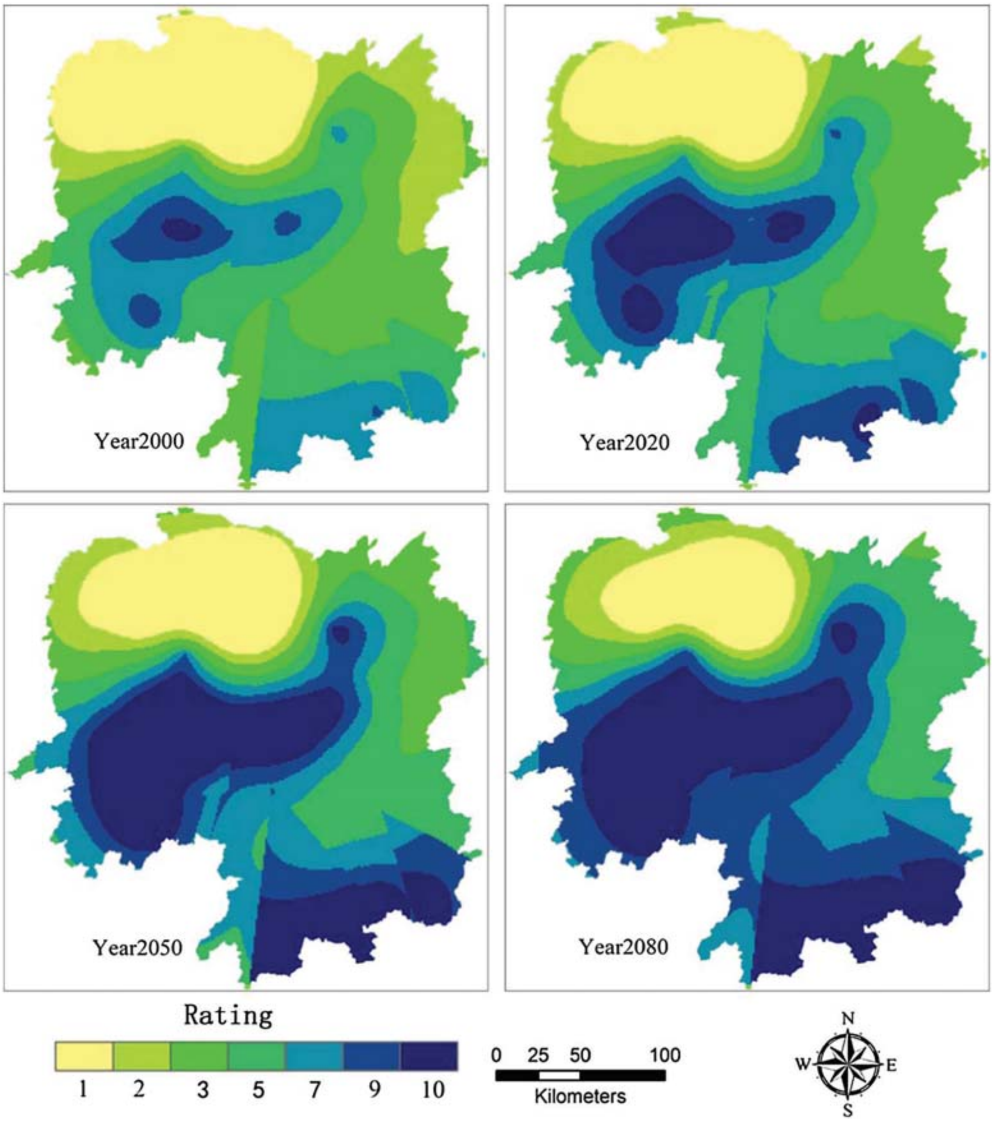

Fig. 4. Distribution of baseline (2000) and projected (2020, 2050, and 2080) depth-to-water table under the climatic change scenarios in Hunan province

Fig. 4 shows the results of future scenarios of mean annual DTW in the study area. The results indicate that climate change could affect DTW strongly in most parts of Hunan province with increases ranging from 2 to 10 m. The projection of DTW predict a state of growth from 2000 to 2080. The average of DTW will reach to 6.38 m in Hunan by 2080. The increase in DTW scenario can be explained by the time projected future precipitation patterns. During the simulated period, increases in net recharge can strongly enhance the amount of water recharged to the aquifer and hence elevate groundwater levels.

The land-use projections indicate that large-scale farmland will be transformed to urban land in the future (Fig. 5). The proportion of urban land will be expected to change from 1.18% in 2000 to 2.95% in 2020, 3.17% in 2050, and 3.39% in 2080. The simulated results indicate that the area of urban land is growing rapidly over time. The greatest increases in urban land are predicted to occur in the Dongting Lake ecoregion, which covers Yueyang City, and Chang-Zhu-Tan ecoregion, which contains Changsha City, Zhuzhou City, and Xiangtan City. Compared with other regions of Hunan province, these two ecoregions feature high population density, convenient transportation, lower elevations, generally warmer temperatures, and abundant water resource, which are considered suitable for urbanization.

Groundwater vulnerability in Hunan Province for the baseline year 2000 and the future year 2020, 2050, and 2080 are calculated (Fig. 6). The vulnerability index is divided into five equal interval classes ranging from very low to very high. In baseline period (year 2000) and future period (year 2020, 2050, and 2080), the eastern and central parts of the Hunan province show high or very high vulnerability, indicating that they are the most vulnerable to external contamination. Nevertheless, the majority of study areas have low or moderate vulnerability, as indicated in the Table 2.

Table 2 presents the results of the increasing trend from low to high vulnerability in the future. The variations from 2000 to 2080 in vulnerability class of low, very low, moderate, high, and very high were −4.76, −20.22, 12.01, 11.61, and 1.36%, respectively. Areas facing potential change covered 52,907 km^2 in Hunan province. Hunan province may face a high risk of groundwater pollution in the future. Groundwater vulnerability patterns are expected to shift significantly under all future scenarios. Specifically, taking the central City Cluster ecoregions as the center, which covers Loudi City, Shaoyang City, and Hengyang City, the groundwater vulnerability classes continually spread to the surrounding countryside. Areas of moderate, high, and very high vulnerability will dramatically expand, and areas of low or very low vulnerability will substantially shrink. Areas with moderate, high, and very-high groundwater

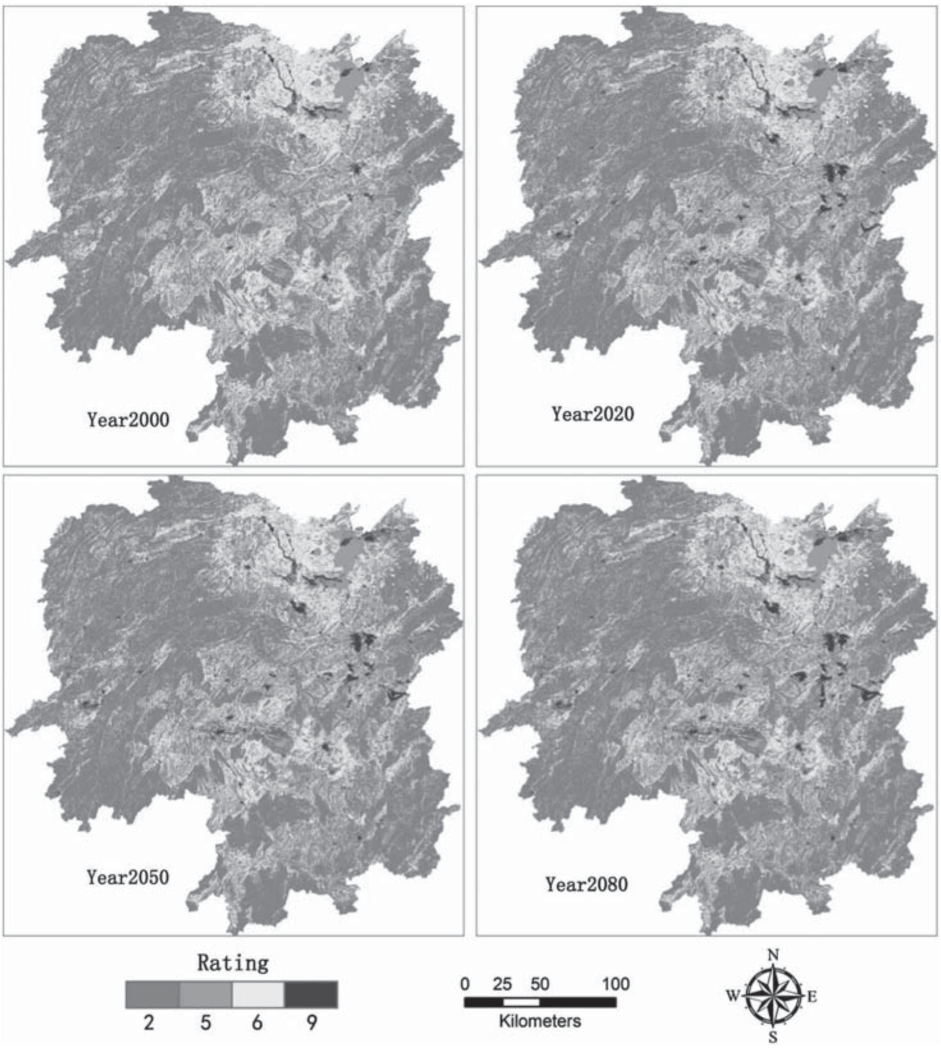

Fig. 5. Distribution of baseline (2000) and projected (2020, 2050, and 2080) urban-related land-use patterns under the climatic change scenarios in Hunan province

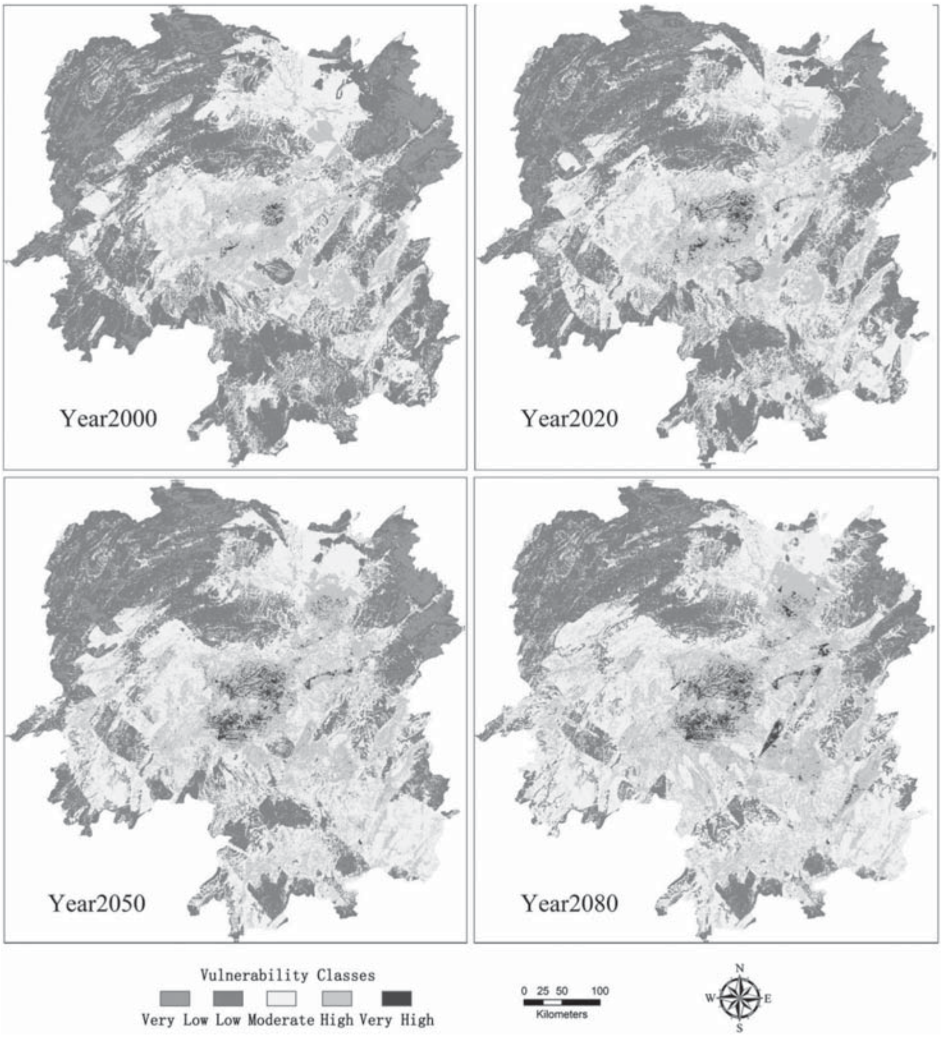

Fig. 6. Distribution of baseline (2000) and projected (2020, 2050, and 2080) groundwater vulnerability under the climatic change scenarios in Hunan province

Table 2. Areas and Percent of Different Vulnerability Classes and Change during the Modeling Period (Unit: 10^3 ha)

	Vulnerability class				
Year/period	Very low	Low	Moderate	High	Very high
Baseline 2000	1,463.81 (6.91%)	10,618.88 (50.14%)	7,564.18 (35.71%)	1,498.69 (7.08%)	34.44 (0.16%)
Year 2020	1,431.61 (6.76%)	9,538.23 (45.03%)	8,141.38 (38.44%)	1,962.73 (9.27%)	106.04 (0.50%)
Year 2050	1,115.94 (5.27%)	7,685.39 (36.28%)	9,262.92 (43.73%)	2,901.08 (13.70%)	214.67 (1.01%)
Year 2080	455.91 (2.15%)	6,335.75 (29.91%)	10,108.78 (47.73%)	3,957.07 (18.68%)	322.49 (1.52%)
Change during 2000–2020	−32.20 (−0.15%)	−1,080.65 (−5.10%)	577.20 (2.73%)	464.04 (2.19%)	71.61 (0.34%)
Change during 2000–2050	−347.87 (−1.64%)	−2,933.49 (−13.85%)	1,698.74 (8.02%)	1,402.39 (6.62%)	180.23 (0.85%)
Change during 2000–2080	−1,007.90 (4.76%)	−4,283.13 (−20.22%)	2,544.6 (12.01%)	2,458.38 (11.61%)	288.06 (1.36%)

pollution potential show the greatest increase under the future scenario. This is most likely attributable to the increase of DTW. The groundwater vulnerability class and DTW have a similar growth trend, as shown in Figs. 6 and 5. Under the future climate change scenarios, both decreases/increases in recharge and DTW will boost factor rating, and together they will have a more-pronounced effect on the increase of groundwater vulnerability. Under the future land-use change scenarios, urban-related land-use patterns contribute to the increase in potential risk of groundwater contamination in future groundwater vulnerability.

A sensitivity analysis was performed to assess how DTW recharge and land-use change could affect groundwater vulnerability in the future. The analysis evaluated overall model responsiveness to the predicted factors using the Eq. (4) (Edet 2014)

$$\theta = \frac{\Delta P_r \times P_w}{VI(x)} \tag{4}$$

where θ = variation of groundwater vulnerability expressed by the factor; $VI(x)$ = final vulnerability index affected by changes

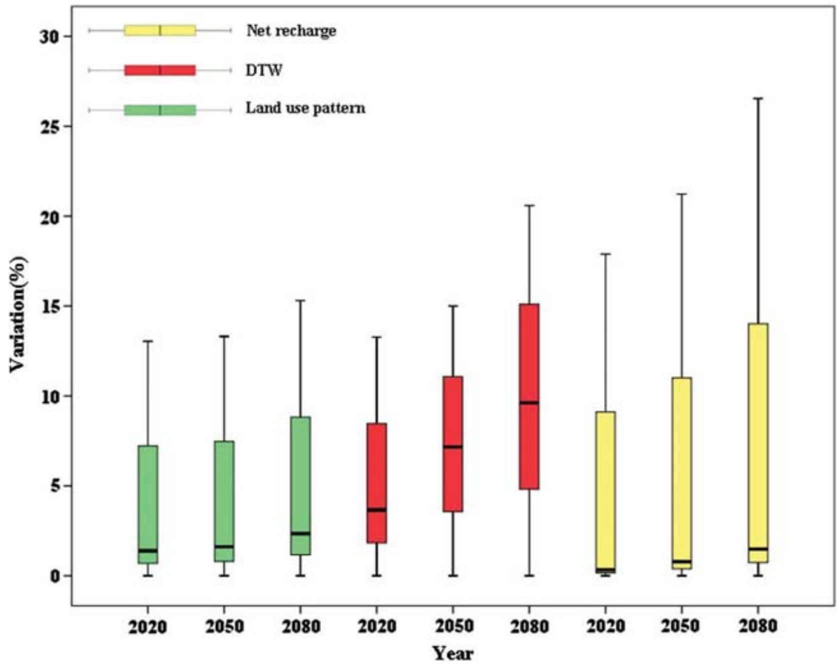

Fig. 7. Sensitivity analysis of change parameters to future groundwater vulnerability

in specific factor x (e.g., DTW and recharge); ΔP_r and P_w = changed rating value and weight of each factor, respectively.

The results reported in Fig. 7 show the smallest, average, and largest variations in groundwater vulnerability in the study area caused by varying net recharge, DTW and land-use patterns. It can be known that the changes in DTW, net recharge, and land use will lead to changes in groundwater vulnerability for 2020, 2050, and 2080. Overall, the variations in groundwater vulnerability caused by changes in DTW are much more significant than those caused by changes in land use and net recharge. The average variations caused by DTW in 2020, 2050, and 2080 are 3.66, 7.15, and 9.62%, respectively. The effects of land use on groundwater vulnerability have the largest contributions. The highest variations caused by land-use patterns will reach to 26.54% by 2080. It is confirmed that the land-use pattern is the most sensitive parameter on the predicted future groundwater vulnerability in Hunan under future scenarios. DTW and land-use pattern have different contributions on the variations of groundwater vulnerability. Greater emphasis should be placed on modeling of the effects of climate change and human activities on future groundwater vulnerability, since the future DTW variations linked to the climate change directly and land-use patterns are also associated with human activities.

Conclusions

This study predicted future groundwater vulnerabilities under an ensemble of climate change scenarios and urban-related land-use change scenarios. Hunan province, in central China, which is undergoing rapid urbanization, was used as an example. The DRASTIC model was used to generate a map of groundwater vulnerability. land-use pattern was considered as an additional DRASTIC parameter. The LTM model was also employed to simulate land-use patterns taking current and future policy driving forces into account. The resulting DRASTIC map showed that the pattern of groundwater vulnerability in Hunan Province would change in the future. Taking the central City Cluster ecoregions as the center, which covers Loudi City, Shaoyang City, and Hengyang City, the groundwater vulnerability classes would continually spread to the surrounding areas. The sensitivity analysis indicated that the DTW may be the dominant factor, and land-use pattern is the most sensitive parameter on the predicted future groundwater vulnerability in Hunan province.

As noted previously, groundwater vulnerability is expected to have higher variations in future periods due to climate change. Meanwhile, groundwater pollution, coupled with urbanization, is likely to cause exacerbate groundwater vulnerability. Thus, groundwater resources managers will likely need to target protection measures such as regulating application of urbanization in areas prone to high groundwater pollution risk. This research could, perhaps, aid groundwater managers in selecting and prioritizing sites for future groundwater monitoring and protection. For areas predicted to have high groundwater vulnerability, appropriate urban policies may be imperative to prevent groundwater contamination. The results from this research may also help to promote dialogue and improve decision-making on urban development, polices, and laws by incorporating groundwater pollution risk and concerns. Although this research was conducted in Hunan province, it clearly could be adapted and applied in other similar regions undergoing significant climate change and rapid land-use change.

Therefore, addressing future groundwater vulnerability characteristics due to future change scenarios and predicting the spatiotemporal variability of water resources are absolutely necessary in making policies to effectively ensure sustainable groundwater resource development. It can also help decision makers to identify potential future groundwater vulnerabilities and take early steps to protect this critical resource.

Acknowledgments

This study was financially supported by the National Natural Science Foundation of China (51521006, 51479072, 51579094, and 51679082), the Program for Changjiang Scholars and Innovative Research Team in University (IRT-13R17), and China Meteorological Data Sharing Service System.

References

Ali, R., et al. (2012). "Potential climate change impacts on groundwater resources of south-western Australia." *J. Hydrol.*, 475(12), 456–472.

Ando, A. W., and Mallory, M. L. (2012). "Optimal portfolio design to reduce climate-related conservation uncertainty in the Prairie Pothole region." *Pnas*, 109(17), 6484–6489.

Babiker, I. S., Mohamed, M. A., Hiyama, T., and Kato, K. (2005). "A GIS-based DRASTIC model for assessing aquifer vulnerability in Kakamigahara Heights, Gifu Prefecture, central Japan." *Sci. Total. Environ.*, 345(1-3), 127–140.

Boy-Roura, M., Mencio, A., and Mas-Pla, J. (2013). "Temporal analysis of spring water data to assess nitrate inputs to groundwater in an agricultural area (Osona, NE Spain)." *Sci. Total. Environ.*, 452–453(5), 433–445.

Chae, G. T., et al. (2004). "Hydrogeochemistry of alluvial groundwaters in an agricultural area: An implication for groundwater contamination susceptibility." *Chemosphere*, 55(3), 369–378.

Chen, S., Wu, W., Hu, K., and Li, W. (2010). "The effects of land-use change and irrigation water resource on nitrate contamination in shallow groundwater at county scale." *Ecol. Complex*, 7(2), 131–138.

Chen, Z. H., Grasby, S. E., and Osadetz, K. G. (2002). "Predicting average annual groundwater levels from climatic variables: An empirical model." *J. Hydrol.*, 260(1–4), 102–117.

China Statistical Yearbook. (2013). "China geo-environment monitoring groundwater levels yearbook." China Land, Beijing (in Chinese).

De Paz, J. M., and Ramos, C. (2002). "Linkage of a geographical information system with the gleams model to assess nitrate leaching in agricultural areas." *Environ. Pollut.*, 118(2), 249–258.

Dimitriou, E., and Moussoulis, E. (2009). "Hydrological and nitrogen distributed catchment modeling to assess the impact of future climate change at Trichonis Lake, western Greece." *Hydrogeol. J.*, 18(2), 441–454.

Edet, A. (2014). "An aquifer vulnerability assessment of the Benin Formation aquifer, Calabar, southeastern Nigeria, using DRASTIC and GIS approach." *Environ. Earth Sci.*, 71(4), 1747–1765.

Fan, T., et al. (2008). "Biosorption of cadmium(ii), zinc(ii) and lead(ii) by Penicillium simplicissimum: Isotherms, kinetics and thermodynamics." *J. Hazard. Mater.*, 160(2–3), 655–661.

Fan, Y., Li, H., and Miguez-Macho, G. (2013). "Global patterns of groundwater table depth." *Science*, 339(6122), 940–943.

Fu, G., Charles, S. P., and Kirshner, S. (2013). "Daily rainfall projections from general circulation models with a downscaling nonhomogeneous hidden Markov model (NHMM) for south-eastern Australia." *Hydrol. Process.*, 27(25), 3663–3673.

Gogu, R. C., and Dassargues, A. (2000). "Current trends and future challenges in groundwater vulnerability assessment using overlay and index methods." *Environ. Geol.*, 39(6), 549–559.

Gong, J. L., et al. (2009). "Removal of cationic dyes from aqueous solution using magnetic multi-wall carbon nanotube nanocomposite as adsorbent." *J. Hazard. Mater.*, 164(2–3), 1517–1522.

Hernandez-Espriu, A., et al. (2014). "The DRASTIC-Sg model: an extension to the DRASTIC approach for mapping groundwater vulnerability in aquifers subject to differential land subsidence, with application to Mexico City." *Hydrogeol. J.*, 22(6), 1469–1485.

Holman, I. P., Dubus, I. G., Hollis, J. M., and Brown, C. D. (2004). "Using a linked soil model emulator and unsaturated zone leaching model to account for preferential flow when assessing the spatially distributed risk of pesticide leaching to groundwater in England and Wales." *Sci. Total. Environ.*, 318(1-3), 73–88.

Hua, S., et al. (2015). "How to manage future groundwater resource of China under climate change and urbanization: An optimal stage investment design from modern portfolio theory." *Water Res.*, 85, 31–37.

Huan, H., Wang, J., and Teng, Y. (2012). "Assessment and validation of groundwater vulnerability to nitrate based on a modified DRASTIC model: A case study in Jilin City of northeast China." *Sci. Total. Environ.*, 440(3), 14–23.

Huang, D. L., et al. (2008). "Degradation of lead-contaminated lignocellulosic waste by Phanerochaete chrysosporium and the reduction of lead toxicity." *Environ. Sci. Technol.*, 42(13), 4946–4951.

Huang, K., Liu, X., Li, X., Liang, J., and He, S. (2013a). "An improved artificial immune system for seeking the Pareto front of land-use allocation problem in large areas." *Int. J. Geog. Inf. Sci.* 27(5), 922–946.

Huang, M., Zhang, W., Jiang, L., and Zou, Y. (2013b). "Impact of temperature changes on early-rice productivity in a subtropical environment of China." *Field Crop. Res.*, 146(146), 10–15.

IPCC Special Report. (2013). "IPCC special report on emissions scenarios: A special report of Working Group III of the Intergovernmental Panel on Climate Change." Cambridge University Press, Cambridge, U.K.

Kraller, G., Warscher, M., Kunstmann, H., Vogl, S., Marke, T., and Strasser, U. (2012). "Water balance estimation in high Alpine terrain by combining distributed modeling and a neural network approach (Berchtesgaden Alps, Germany)." *Hydrol. Earth Syst. Sci.*, 16(7), 1969–1990.

Kumar, S., Thirumalaivasan, D., and Radhakrishnan, N. (2014). "GIS based assessment of groundwater vulnerability using drastic model." *Arab. J. Sci. Eng.*, 39(1), 207–216.

Kura, N. U., et al. (2015). "Assessment of groundwater vulnerability to anthropogenic pollution and seawater intrusion in a small tropical island using index-based methods." *Environ. Sci. Pollut. Res.*, 22(2), 1512–1533.

Lapworth, D. J., et al. (2013). "Residence times of shallow groundwater in West Africa: Implications for hydrogeology and resilience to future changes in climate." *Hydrogeol. J.*, 21(3), 673–686.

Li, R., and Merchant, J. W. (2013). "Modeling vulnerability of groundwater to pollution under future scenarios of climate change and biofuels-related land-use change: A case study in North Dakota, USA." *Sci. Total. Environ.*, 447(1), 32–45.

Li, X. D., et al. (2015). "The application of semicircular-buffer-based land-use regression models incorporating wind direction in predicting quarterly NO_2 and PM_{10} concentrations." *Atmos. Environ.*, 103, 18–24.

Liang, J., et al. (2010). "Optimal solute transport in heterogeneous aquifer: Coupled inverse modelling." *Int. J. Environ. Pollut.*, 42(1–3), 258–269.

Liang, J., et al. (2015). "Facile synthesis of alumina-decorated multi-walled carbon nanotubes for simultaneous adsorption of cadmium ion and trichloroethylene." *Chem. Eng. J.*, 273, 101–110.

Liu, W., et al. (2015). "land-use regression models coupling with meteorology to model spatial and temporal variability of NO_2 and PM_{10} in Changsha, China." *Atmos. Environ.*, 116, 272–280.

Masetti, M., Sterlacchini, S., Ballabio, C., Sorichetta, A., and Poli, S. (2009). "Influence of threshold value in the use of statistical methods for groundwater vulnerability assessment." *Sci. Total. Environ.*, 407(12), 3836–3846.

National Climate Center of China. "The CGIAR consortium for spatial information." ⟨http://ncc.cma.gov.cn/cn/⟩.

Neukum, C., and Azzam, R. (2012). "Impact of climate change on groundwater recharge in a small catchment in the Black Forest, Germany." *Hydrogeol. J.*, 20(3), 547–560.

Pasini, S., Torresan, S., Rizzi, J., Zabeo, A., Critto, A., and Marcomini, A. (2012). "Climate change impact assessment in Veneto and Friuli Plain groundwater. Part II: A spatially resolved regional risk assessment." *Sci. Total. Environ.*, 447(1), 219–235.

Pijanowski, B. C., Brown, D. G., Shellito, B. A., and Manik, G. A. (2002). "Using neural networks and GIS to forecast land-use changes: A land transformation model." *Comput. Environ. Urban Sys.*, 26(6), 553–575.

Rahman, A. (2008). "A GIS based DRASTIC model for assessing groundwater vulnerability in shallow aquifer in Aligarh, India." *Appl. Geog.*, 28(1), 32–53.

Raupach, M. R., Haverd, V., and Briggs, P. R. (2013). "Sensitivities of the Australian terrestrial water and carbon balances to climate change and variability." *Agric. Forest Meteorol.*, 182–183(12), 277–291.

Şen, Z., Alsheikh, A., Al-Turbak, A. S., Al-Bassam, A. M., and Al-Dakheel, A. M. (2013). "Climate change impact and runoff harvesting in arid regions." *Arab. J. Geosci.*, 6(1), 287–295.

Shirazi, S. M., Imran, H. M., Akib, S., Yusop, Z., and Harun, Z. B. (2013). "Groundwater vulnerability assessment in the Melaka State of Malaysia using DRASTIC and GIS techniques." *Environ. Earth Sci.*, 70(5), 2293–2304.

Snover, A. K., Mantua, N. J., Littell, J. S., Alexander, M. A., McClure, M. M., and Nye, J. (2013). "Choosing and using climate-change scenarios for ecological-impact assessments and conservation decisions." *Conserv. Biol.*, 27(6), 1147–1157.

Stigter, T. Y., et al. (2014). "Comparative assessment of climate change and its impacts on three coastal aquifers in the Mediterranean." *Reg. Environ. Change*, 14(S1), 41–56.

Tang, L., Zeng, G. M., Shen, G. L., Li, Y. P., Zhang, Y., and Huang, D. L. (2008). "Rapid detection of picloram in agricultural field samples using a disposable immunomembrane-based electrochemical sensor." *Environ. Sci. Technol.*, 42(4), 1207–1212.

Wang, J., He, J., and Chen, H. (2012). "Assessment of groundwater contamination risk using hazard quantification, a modified DRASTIC model and groundwater value, Beijing Plain, China." *Sci. Total. Environ.*, 432(16), 216–226.

Wu, W., Yin, S., Liu, H., and Chen, H. (2014). "Groundwater vulnerability assessment and feasibility mapping under reclaimed water irrigation by a modified DRASTIC model." *Water Resour. Manag.*, 28(5), 1219–1234.

Xu, P., et al. (2012). "Use of iron oxide nanomaterials in wastewater treatment: A review." *Sci. Total Environ.*, 424(4), 1–10.

Yuan, F., et al. (2010). "Adsorption of cd (ii) and zn (ii) from aqueous solutions using magnetic hydroxyapatite nanoparticles as adsorbents." *Chem. Eng. J.*, 162(2), 487–494.

Zeng, G. M., et al. (2009). "Spatial analysis of human health risk associated with ingesting manganese in Huangxing Town, Middle China." *Chemosphere*, 77(3), 368–375.

Zeng, G. M., Chen, M., and Zeng, Z. T. (2013a). "Risks of neonicotinoid pesticides." *Science*, 340(6139), 1403.

Zeng, G. M., Chen, M., and Zeng, Z. T. (2013b). "Shale gas: Surface water also at risk." *Nature*, 499(7457), 154.